NURETH14-067

NUMERICAL SIMULATION OF COUNTERCURRENT GAS-LIQUID FLOW IN A PWR HOT LEG USING VOF METHOD

M. Murase[1], I. Kinoshita[1], C. Yanagi[1], Y. Utanohara[1], T. Takata[2], A. Yamaguchi[2] and A. Tomiyama[3]
[1] Institute of Nuclear Safety System, Inc., Fukui, Japan
[2] Osaka University, Osaka, Japan
[3] Kobe University, Kobe, Japan

Abstract

In order to evaluate flow patterns and CCFL (countercurrent flow limitation) characteristics in a PWR hot leg under reflux condensation, numerical simulations have been done using a two-fluid model and a VOF (volume of fluid) method implemented in the CFD software, FLUENT6.3.26. The two-fluid model gave good agreement with CCFL data under low pressure conditions but did not give good results under high pressure steam-water conditions. On the other hand, the VOF method gave good agreement with CCFL data for tests with a rectangular channel but did not give good results for calculations in a circular channel. Therefore, in this paper, the computational grid and schemes were changed in the VOF method, numerical simulations were done for steam-water flows at 1.5 MPa under PWR full-scale conditions with the inner diameter of 0.75 m, and the calculated results were compared with the UPTF data at 1.5 MPa. As a result, the calculated flow pattern was found to be similar to the flow pattern observed in small-scale air-water tests, and the calculated CCFL characteristics agreed well with the UPTF data at 1.5 MPa except in the region of a large steam volumetric flux.

Introduction

Reflux condensation by a steam generator (SG) is considered as one of the possible core cooling methods under hypothetical accident conditions in a pressurized water reactor (PWR). In the reflux condensation, the steam generated in the core and the water condensed in the SG form a countercurrent flow in a hot leg, which consists of a horizontal pipe, an elbow and an inclined pipe. Several experiments have been conducted to investigate the countercurrent flow limitation (CCFL) in the hot leg [1-6], and empirical correlations were proposed using Wallis parameters [7]. Experiments under high pressure steam-water or full-scale conditions, however, are limited and effects of the shape and size of the flow channel and fluid properties on flow patterns and CCFL characteristics are not well understood. In order to evaluate these effects better, numerical simulation using CFD (computational fluid dynamics) software is expected to be useful. Wang and Mayinger [8] conducted two-dimensional calculations of countercurrent flow in the hot leg of the UPTF tests [4] using a two-fluid model. However, they assigned boundary conditions at the inlet and outlet of the hot leg which might affect the predicted flow patterns in the hot leg, and CCFL characteristics can not be calculated using boundary conditions given at the inlet and outlet of the hot leg.

In order to investigate detailed flow patterns in the hot leg under countercurrent gas-liquid flow conditions, countercurrent air-water tests were conducted at Kobe University using a 1/5-scale rectangular channel [9] and a 1/15-scale circular channel [10] simulating a PWR hot leg. CCFL characteristics were measured, and flow patterns were observed in the horizontal, elbow and inclined sections. Numerical simulations of the tests using a two-fluid mode implemented in the CFD software, FLUENT6.3.26, were also done [11, 12]. The predicted flow patterns in the hot leg were similar to the observed results, and calculated results agreed well with CCFL data. Moreover, numerical simulations for the PWR plant conditions were made using the two-fluid model, and it was confirmed that CCFL characteristics in the hot leg could be well correlated with the Wallis parameters for system pressures below 0.3 MPa [13]. The two-fluid model, however, did not give good results for high pressures over 1.5 MPa. Therefore, in order to evaluate the effects of system pressures and fluid properties on CCFL characteristics, a VOF (volume of fluid) method was applied and validated using data in the 1/5-scale rectangular channel [14]. The VOF method, however, could not well simulate CCFL characteristics in the 1/15-scale circular channel [15].

In this paper, in order to apply the VOF method to calculations of CCFL characteristics in a circular channel, the computational grid and schemes were changed in the VOF method used in the previous study [15]. Numerical simulations were conducted for steam-water flows at 1.5 MPa under PWR full-scale conditions with the inner diameter of 0.75 m, and the calculated results were compared with the UPTF data [4] at 1.5 MPa. It should be noted that the objective of this study is not validation of a CFD software nor a benchmark calculation of countercurrent flow but to find out a practical method for parameter calculations.

1. Outline of previous simulations

In numerical simulations, an Euler-Euler model (i.e. two-fluid model) or a VOF method implemented in the CFD software, FLUENT6.3.26 was used. The standard $k-\varepsilon$ turbulent model was used for gas and liquid phases in order to simulate turbulent velocity distributions. On wall surfaces, conditions of non-slip and the standard wall function were used. Momentum, volume fraction, turbulent kinetic energy and turbulent dissipation rate of gas and liquid phases were calculated using the first order upwind scheme. The phase-coupled-SIMPLE method was used for the pressure-velocity coupling.

In order to evaluate CCFL characteristics, the calculation region included the lower tank simulating the upper plenum in a pressure vessel and the upper tank simulating the SG inlet plenum. From the increasing rate of water mass in the lower tank, the falling water flow rate through the hot leg was obtained. Then the relationship between the gas flow rate and the falling water flow rate was arranged using the Wallis parameters [7]:

$$J_k^{\ *} = J_k \left\{ \frac{\rho_k}{g \cdot D_h \left(\rho_L - \rho_G \right)} \right\}^{1/2}, \ (k = G \text{ or } L) \qquad (1)$$

where D_h is the hydraulic diameter of the hot leg, g [m/s^2] is gravity acceleration, J [m/s] is the volumetric flux in the hot leg, and ρ [kg/m^3] is density.

1.1 Two-fluid model

In the two-fluid model, a user function was employed to calculate the interfacial drag between gas and liquid phases. A combination of three correlations for the interfacial drag coefficients, ($C_D A_i$), including the interfacial area concentration, A_i [m^2/m^3], as a function of local void fractions, was used. The proposed combination of correlations was validated using CCFL data in the 1/5-scale rectangular channel [9] and the 1/15-scale circular channel [10], and the simulated results agreed well with the data [11, 12]. Moreover, numerical simulations for the PWR plant conditions were conducted using the two-fluid model and the same combination of correlations for the interfacial drag coefficients [13].

Figure 1 summarizes the simulation results. In the UPTF tests [4], the inner diameter of the hot leg was D = 0.75 m. However, the hydraulic diameter of D_h = 0.65 m in the region with the ECC (emergency core cooling) injection tube was used in Eq. (1) because flooding might occur in the region. The relationship between J_G and J_L strongly depended on the hydraulic diameter of the hot leg and fluid properties as shown in Fig. 1 (a). However, CCFL characteristics arranged by the Wallis parameters agreed well each other as shown in Fig. 1 (b). The results shown in Fig. 1 indicated that Wallis parameters expressed by Eq. (1) and the proposed combination of correlations for the interfacial drag coefficients in the two-fluid model were valid for different diameters and fluid properties under low pressures below 0.3 MPa.

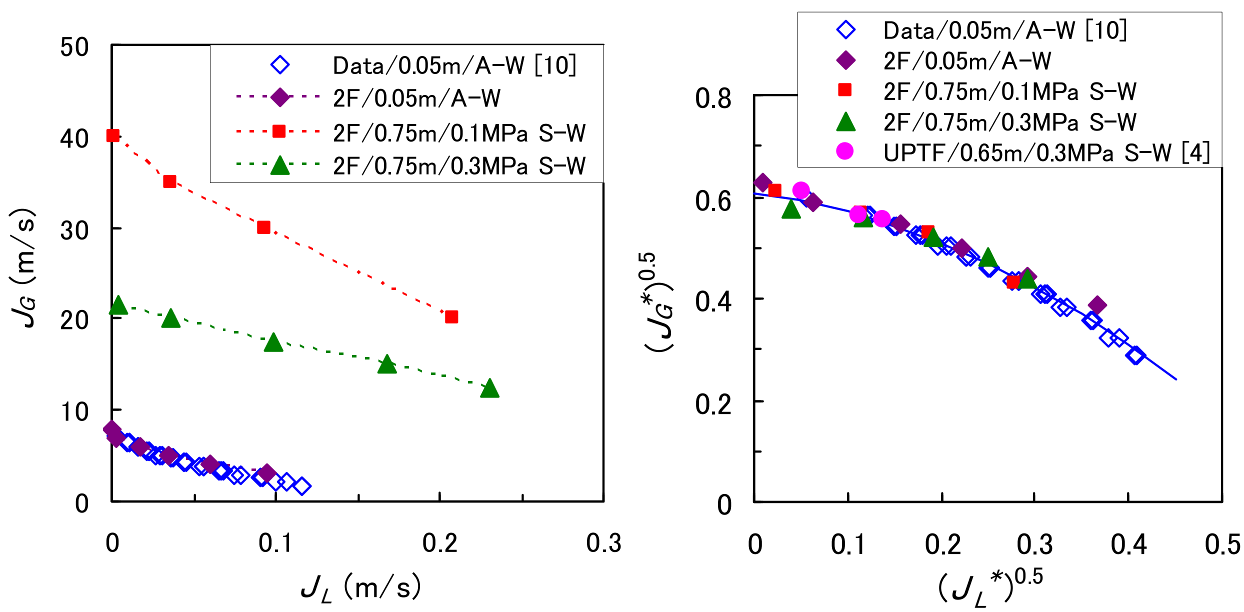

(a) Relationship between J_G and J_L　　(b) CCFL characteristics

Figure 1　Calculated CCFL characteristics (2F, two-fluid; A-W, air-water; S-W, steam-water).

CCFL points calculated for 1.5 MPa using the two-fluid model were below the fitted curve in Fig. 1 (b). This may be because most of the correlations for the interfacial drag coefficients used in the two-fluid model were derived using mainly air-water data. At present, it is not easy to modify them for high pressure steam-water conditions due to lack of data.

1.2 VOF method

The VOF method has a benefit that empirical correlations are not needed. In numerical simulations using the VOF method, the same computational grid and schemes as the two-fluid model were used except for the two-phase flow model.

Figure 2 compares CCFL characteristics calculated by the VOF method [11, 14] with the data in the 1/5-scale rectangular channel simulating a PWR hot leg [9, 14]. For a rectangular channel, the channel height is generally used for the characteristic length in the Wallis parameters, Eq. (1), instead of the hydraulic diameter. Therefore, in Fig. 2, the channel height of 150 mm was used in the Wallis parameters. In Fig. 2 (a), the two-fluid model overestimated (J_L^*), but the VOF method gave good agreement with the data. In Fig. 2 (b), the VOF method gave good predictions for the air-glycerol 60 wt% solution with large liquid viscosity and the same trend for high pressure steam-water with large gas density and low liquid viscosity as the UPTF data. Therefore, it was expected that the VOF method would give good predictions for effects of fluid properties on CCFL characteristics.

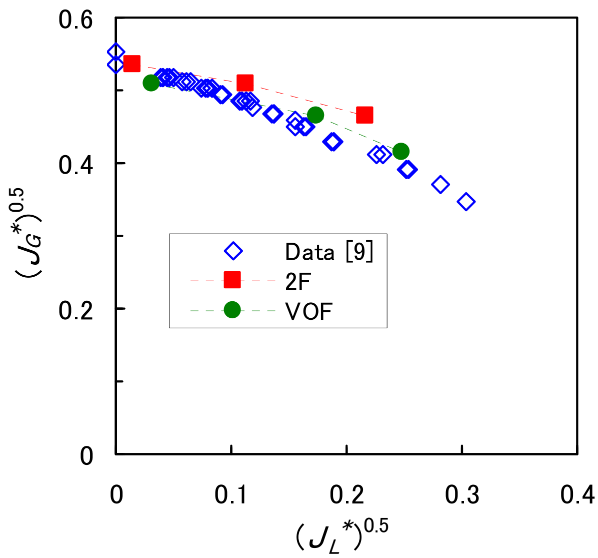

(a) Air-water conditions

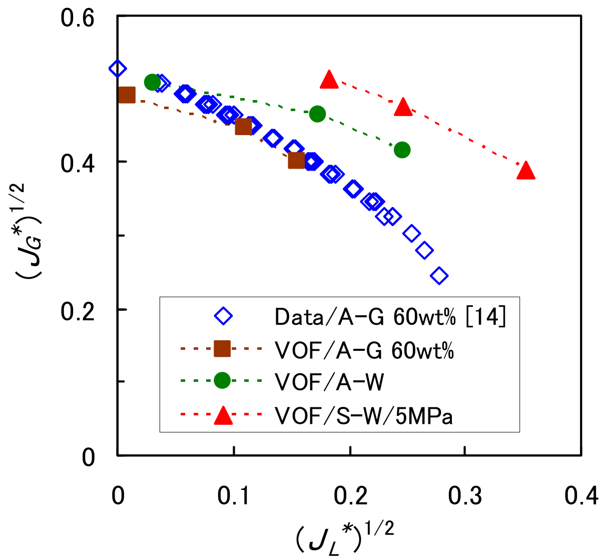

(b) Effects of fluid properties

Figure 2 CCFL characteristics in the 1/5-scale rectangular channel (2F, two-fluid model; VOF, VOF method; A-G, air-glycerol solution; A-W, air-water; S-W, steam-water).

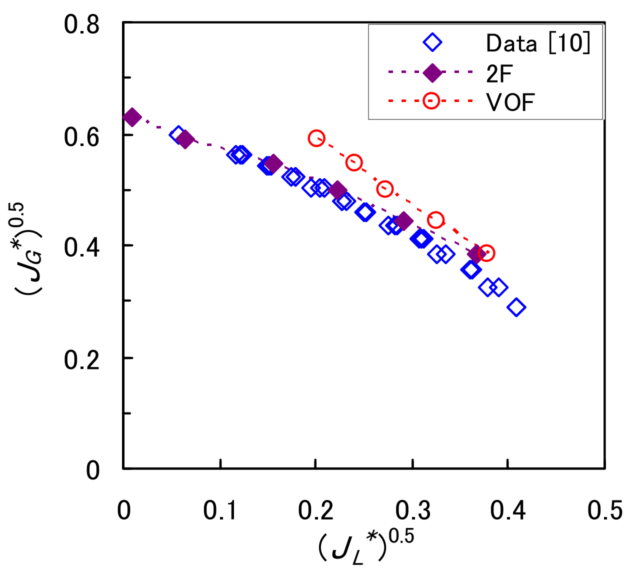

Figure 3 CCFL characteristics in the 1/15-scale circular channel (2F, two-fluid model; VOF, VOF method).

Figure 3 compares CCFL characteristics calculated by the VOF method [15] with the data in the 1/15-scale circular channel simulating a PWR hot leg [10] and results calculated by the two-fluid model [12]. Calculation conditions using the VOF method were basically the same as the calculation conditions using the two-fluid model. Therefore, the mesh sizes might be too large for the VOF method. In the FLUENT-VOF method, the interface shape reproduced by the geometric reconstruction (piecewise-linear) scheme was used for the gas-liquid interface. In the VOF method, the effect of surface tension was not used in this calculation. A laminar flow model was used for gas and liquid phases, because calculations by a turbulent model were unstable and required short time steps. Moreover, the turbulent model greatly underestimated water flow rates through the hot leg. Because of the laminar flow model, the VOF method generally overestimated J_L^*, especially in the region of high J_G^*.

2. Improvement of VOF calculations

As discussed above, the VOF method could be expected to predict effects of system pressures and fluid properties on CCFL characteristics, but could not give good predictions of CCFL characteristics in a circular channel. Therefore, the computational grid and schemes were improved to better calculate CCFL characteristics in a circular channel.

2.1 Computational grid

Figure 4 shows the original computational grid for a PWR hot leg, which was based on the 1/15-scale air-water tests [10]. Because velocity distributions of gas and liquid at both ends of the hot leg affect hydraulic behavior, the calculation region included the lower tank simulating the upper plenum in the reactor vessel and the upper tank simulating the SG inlet plenum. The expansion of the inclined pipe was not simulated in the tests but was simulated in the grid shown in Fig. 4. The number of calculation cells in a cross section of the hot leg was 178 and the total number of calculation cells was about 65,000 in case of normal cells. Fine cells with 460 cells in the cross section were also used in order to examine the effects of the cell size, and it was confirmed that no significant difference appeared in the calculated CCFL characteristics [16]. The diameter of the hot leg and the length of the horizontal pipe were D = 50 mm and L = 430 mm in the 1/15-scale air-water tests (L/D = 8.6). Gas was supplied into the lower tank through a pipe and flowed into the upper tank through the hot leg. Water was supplied from the bottom of the upper tank. Some water gravitationally flowed into the lower tank through the hot leg. The water flow rate through the hot leg was calculated from the increasing rate of water volume in the lower tank. The rest of the water, which did not flow into the lower tank, overflowed the barrage in the upper tank and flowed out with gas through the mixture outlet. The boundary condition of constant velocity was used at the inlets of gas and water, and the boundary condition of constant pressure was used at the outlet of the gas-water mixture.

Figure 5 shows the improved computational grid. In calculations for full-scale PWR conditions, gas velocity in the hot leg became large as shown in Fig. 1 (a), and the gas inlet velocity in the original grid shown in Fig. 4 was about 100 m/s. The high speed gas jet might affect distributions of gas velocity at the gas inlet and inside of the hot leg. Then, in the VOF calculations, the flow pattern observed in the actual tests was not calculated using the original grid. Therefore, in the improved grid, the area of the gas inlet was broadened as shown in Fig. 5. Compared with the normal cell of the original grid, the number of calculation cells was reduced in the lower and upper tanks but was increased in a cross section of the hot leg. In a cross section, the numbers of calculation cells were mainly increased near the pipe wall. As the result, the number of calculation cells in a cross section of the hot leg was raised to 299 and the total number of calculation cells was about 59,000. The cell height near the pipe wall was almost the same as that in the fine cell of the original grid.

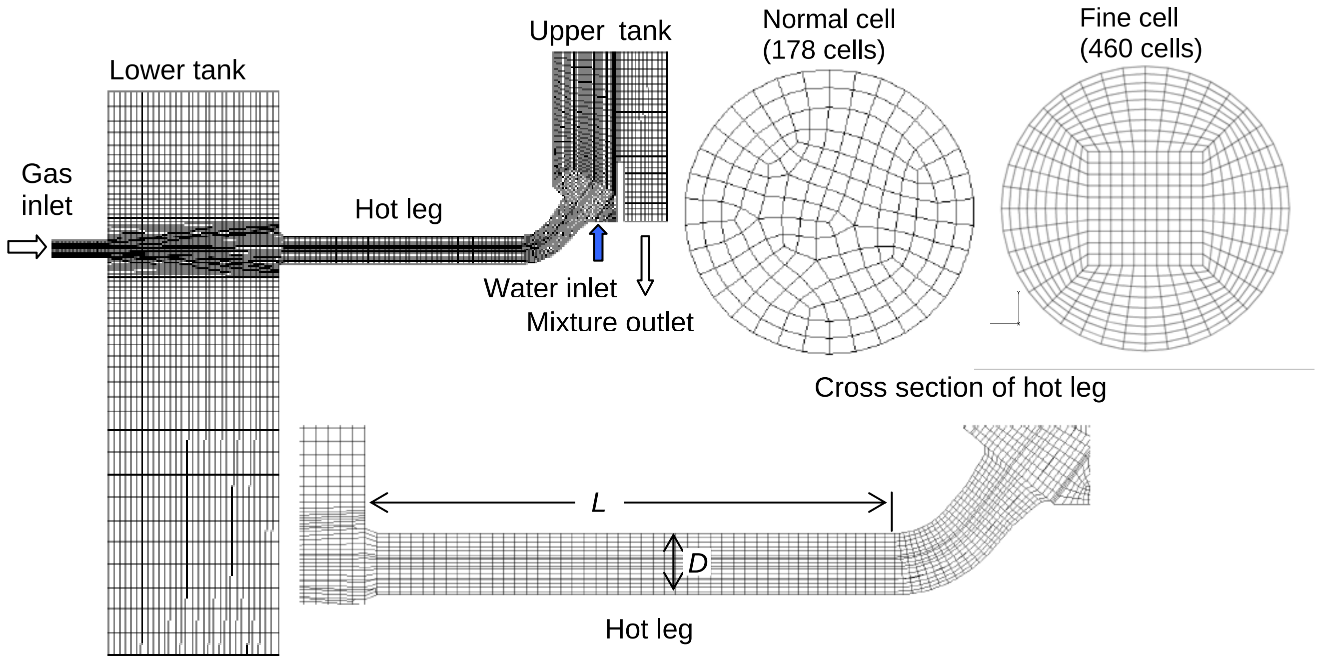

Figure 4 Original computational grid.

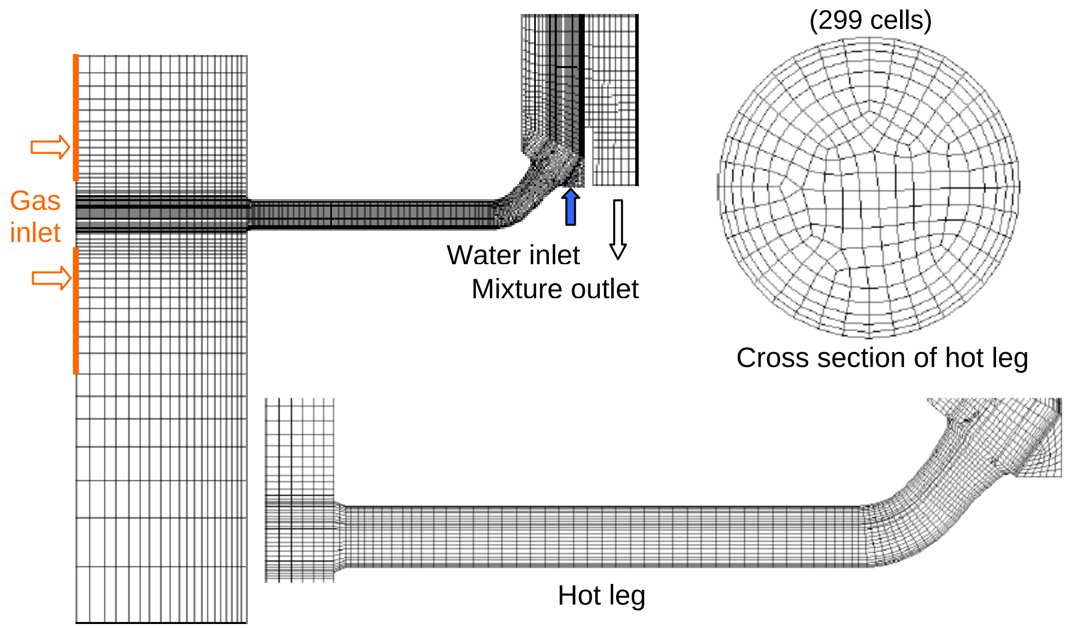

Figure 5 Improved computational grid.

2.2 Computational schemes

In calculations with the original grid, the phase-coupled-SIMPLE method was used for the pressure-velocity coupling and the time step was constant at 0.5-2 ms depending on stability of calculations. Calculations were unstable especially at low pressure conditions with a large density ratio between liquid and gas phases, and sometimes stopped even at a time step of 0.5 ms. Therefore, in calculations with the improved grid, PISO implemented in FLUENT, the non-iterative time advancement with the neighbor correction of 3, and the variable time step were used. Figure 6 shows an example of control panels in FLUENT. Due to the non-iterative time advancement and the variable time step, the calculation time was less than 1/10 of the calculation time before.

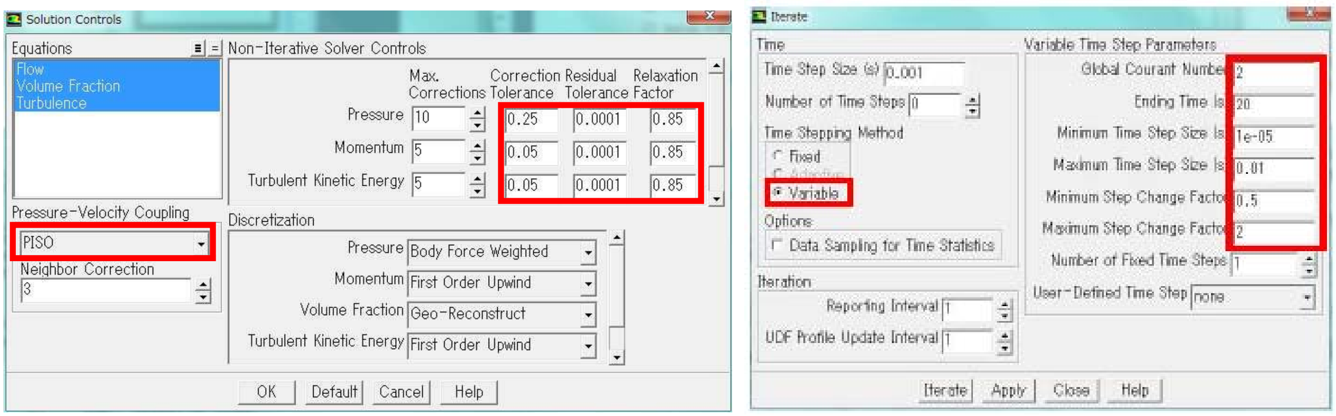

Figure 6 Example of control panels.

3. Calculated results

In numerical simulations, the VOF method implemented in the CFD software, FLUENT6.3.26, was used. The standard $k-\varepsilon$ turbulent model was used for gas and liquid phases in order to simulate turbulent velocity distributions. On wall surfaces, conditions of non-slip and the standard wall function were used. Momentum, volume fraction, turbulent kinetic energy and turbulent dissipation rate of gas and liquid phases were calculated using the first order upwind scheme. The PISO method was used for the pressure-velocity coupling. The maximum value of the turbulent viscosity ratio is 10^5 in the default values of FLUENT. However, the maximum value of 10^4 was used to get good agreement with the UPTF data [4]. Numerical simulations were done for steam-water flows at 1.5 MPa under PWR full-scale conditions with the inner diameter of 0.75 m, and the calculated results were compared with the UPTF data [4] at 1.5 MPa.

3.1 Flow patterns

Figure 7 compares flow patterns calculated by the VOF method with a flow pattern observed in the 1/15-scale air-water tests [10]. Under flooding conditions in the tests, the water flow rate was restricted at the elbow side of the horizontal pipe. In the elbow and inclined pipe, large waves with droplets periodically flowed upward, water flowed downward from the upper tank, and recirculation of water with bubbles and droplets formed. Therefore, the observed test flow pattern fluctuated in the elbow and inclined pipe. The calculation conditions were for steam-water at 1.5 MPa in a full-scale hot leg and different from the test conditions. However the calculated flow patterns were similar to the observed test flow pattern. Stable stratified flow formed in the horizontal pipe because small waves could not be calculated with the rather large calculation cells used. A large wave periodically appeared near the elbow and the water flow rate was restricted there. The large wave flowed into the elbow and the water depth fluctuated in the elbow and the inclined pipe. With increasing J_G, water depth became shallow in the horizontal section.

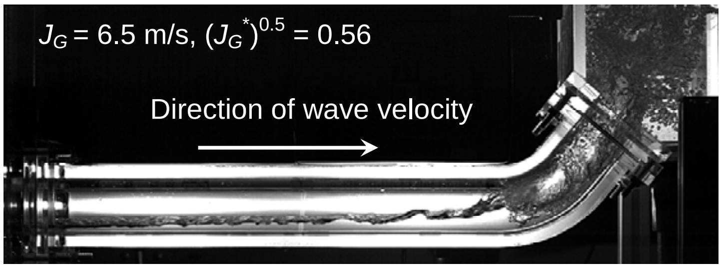

(a) D = 50 mm, air-water test [10]

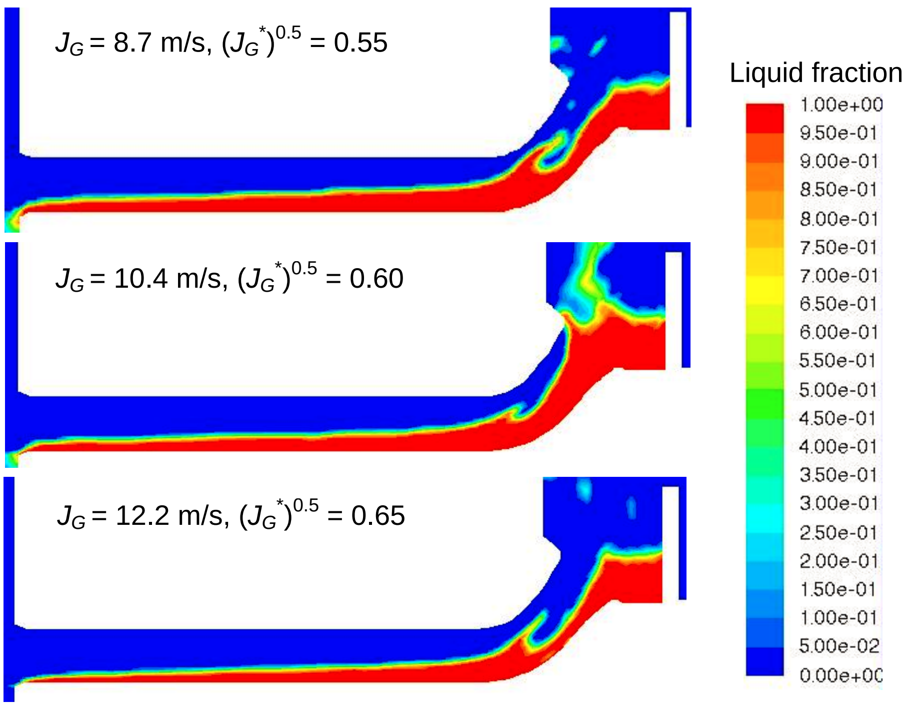

(b) D = 750 mm, steam-water at 1.5 MPa

Figure 7 Flow patterns.

3.2 CCFL characteristics

Figure 8 shows the calculated water volume in the lower tank after the quasi-steady state, which was used to obtain the time-averaged water flow rate through the hot leg. The results during the initial 20-30 s of the calculation were not used because they included transient effects after the change of calculation conditions.

Figure 9 compares the calculated CCFL characteristics with the UPTF data [4]. In the UPTF tests, the inner diameter of the hot leg was D = 0.75 m. However, the hydraulic diameter of D_h = 0.65 m in the region with the ECC injection tube was used in Eq. (1) because flooding might occur in the region. The calculated results agreed very well with the data except for (J_L^*) at high (J_G^*). Therefore, it might be possible to evaluate effects of system pressures and fluid properties on CCFL characteristics using the VOF method.

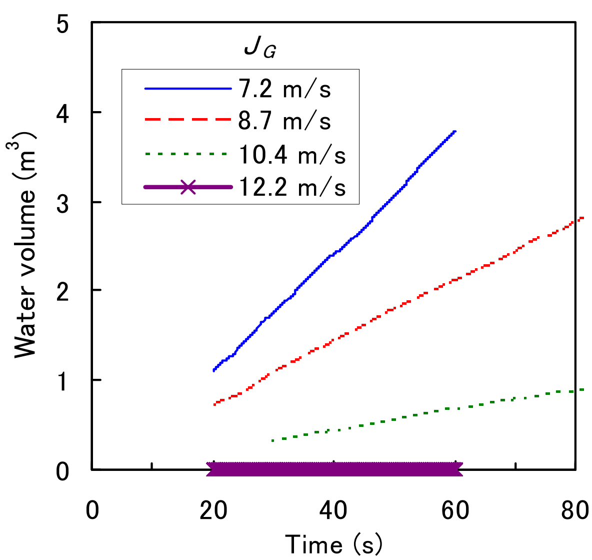

Figure 8 Water volume in lower tank.

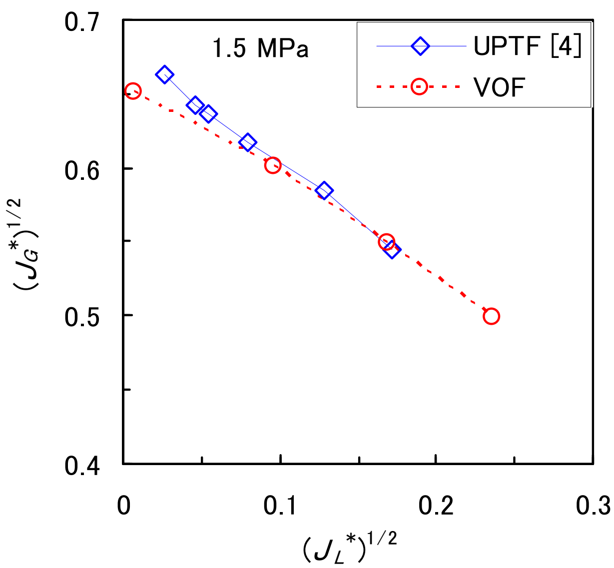

Figure 9 CCFL characteristics at 1.5 MPa.

3.3 Discussion

The calculated results agreed very well with the CCFL data except for (J_L^*) at high (J_G^*) as shown in Fig. 9. In the calculations, however, the maximum value of 10^4 for the turbulent viscosity ratio was used, because the default value of 10^5 in FLUENT remarkably underestimated the falling water flow rate through the hot leg. One of the reasons for the underestimation may be due to the large-size calculation cells used. Calculations with small-size calculation cells greatly increase the computer load and may not be realistic for parameter calculations. Therefore, using the current calculation conditions, effects of system pressures and fluid properties on CCFL characteristics will need to be evaluated in a future study.

4. Conclusion

In this study, the computational grid and schemes were changed in the VOF method used in the previous study to apply the VOF method to CCFL calculations in a full-scale PWR hot leg. Numerical simulations were made for steam-water flows at 1.5 MPa under PWR full-scale conditions with the hot leg pipe inner diameter of 0.75 m, and the calculated results were compared with the UPTF data at 1.5 MPa.

Compared with the original computational grid, the area of the gas inlet was broadened, and the number of calculation cells was reduced in the lower and upper tanks but was increased in a cross section of the hot leg. Then the total number of calculation cells was reduced. The pressure-velocity coupling was changed from the SIMPLE method to the PISO method, the iterative time advancement of 30 times was changed to the non-iterative time advancement with the neighbor correction of 3, and the time step was changed from a constant value to the variable time step. Due to the non-iterative time advancement and the variable time step, the calculation time became less than 1/10 of the calculation time before in the calculations for steam-water at 1.5 MPa.

The maximum value of 10^4 for the turbulent viscosity ratio was used, because the default value of 10^5 in FLUENT remarkably underestimated the falling water flow rate through the hot leg. As the result, the calculated CCFL characteristics agreed very well with the UPTF data except for (J_L^*) at high (J_G^*). Therefore, effects of system pressures and fluid properties on CCFL characteristics will be evaluated in a future study using the current calculation conditions.

5. References

[1] H.J. Richter, G.B. Wallis, K.H. Carter and S.L. Murphy, "Deentrainment and Countercurrent Air-water Flow in a Model PWR Hot-leg", NRC-0193-9, U.S. Nuclear Regulatory Commission, 1978.

[2] A. Ohnuki, "Experimental Study of Counter-Current Two-Phase Flow in Horizontal Tube connected to an Inclined Riser", J. of Nuclear Science Technology, Vol. 23, No. 3, 1986, pp. 219-232.

[3] A. Ohnuki, H. Adachi and Y. Murao, "Scale Effects on Countercurrent Gas-Liquid Flow in a Horizontal Tube Connected to an Inclined Riser", Nuclear Engineering and Design, Vol. 107, 1988, pp. 283-294.

[4] F. Mayinger, P. Weiss, and K. Wolfert, "Two-phase flow phenomena in full-scale reactor geometry", Nuclear Engineering and Design, Vol. 145, 1993, pp. 47-61.

[5] S. Wongwises, "Two-phase countercurrent flow in a model of a pressurized water reactor hot leg", Nuclear Engineering and Design, Vol. 166, 1996, pp. 121-133.

[6] M.A. Navarro, "Study of countercurrent flow limitation in a horizontal pipe connected to an inclined one", Nuclear Engineering and Design, Vol. 235, 2005, pp. 1139-1148.

[7] G.B. Wallis, One-dimensional Two-phase Flow, McGraw Hill, New York, 1969, pp. 320-339.

[8] M.J. Wang and F. Mayinger, "Simulation and analysis of thermal-hydraulic phenomena in a PWR hot leg related to SBLOCA", Nuclear Engineering and Design, Vol. 155, 1995, pp. 643-652.

[9] N. Minami, D. Nishiwaki, H. Kataoka, et al., "Countercurrent Gas-Liquid Flow in a Rectangular Channel Simulating a PWR Hot Leg (1); Flow Pattern and CCFL Characteristics", Japanese J. of Multiphase Flow, Vol. 22, No. 4, 2008, pp. 403-412. [in Japanese]

[10] N. Minami, D. Nishiwaki, T. Nariai, et al., "Countercurrent Gas-Liquid Flow in a PWR Hot Leg under Reflux Cooling (I) Air-Water Tests for 1/15th Scale Model of a PWR Hot Leg", J. of Nuclear Science Technology, Vol. 47, No. 2, 2010, pp. 142-148.

[11] N. Minami, M. Murase, D. Nishiwaki, et al., "Countercurrent Gas-Liquid Flow in a Rectangular Channel Simulating a PWR Hot Leg (2); Analytical Evaluation of Countercurrent

Flow Limitation", Japanese J. of Multiphase Flow, Vol. 22, No. 4, 2008, pp. 413-422. [in Japanese]

[12] N. Minami, M. Murase and A. Tomiyama, "Countercurrent Gas-Liquid Flow in a PWR Hot Leg under Reflux Cooling (II) Numerical Simulation of 1/15-Scale Air-Water Tests", J. of Nuclear Science Technology, Vol. 47, No. 2, 2010, pp. 149-155.

[13] I. Kinoshita, M. Murase, Y. Utanohara, et al., "Numerical Simulation of Countercurrent Gas-Liquid Flow in a PWR Hot Leg under Reflux Cooling", J. of Nuclear Science Technology, Vol. 47, No. 10, 2010, pp. 963-972.

[14] I. Kinoshita, M. Murase, T. Nariai, et al., "Countercurrent Gas-Liquid Flow in a Rectangular Channel Simulating a PWR Hot Leg (3); Evaluation of Effects of Fluid Properties using VOF Method", Japanese J. of Multiphase Flow, Vol. 24, No. 4, 2010, pp. 445-453. [in Japanese]

[15] M. Murase, Y. Utanohara, I. Kinoshita, et al., "Numerical Calculations on Countercurrent Air-Water Flow in Small-Scale Models of a PWR Hot Leg Using a VOF Model", Proceedings of the 17th International Conference on Nuclear Engineering, ICONE17-75116, Brussels, Belgium, 2009 July 12-16.

[16] Y. Utanohara, I. Kinoshita, M. Murase, et al., "Numerical simulation using CFD software of countercurrent gas-liquid flow in a PWR hot leg under reflux condensation", Nuclear Engineering and Design, Vol. 241, 2011, pp. 1643-1655.